

AN EXPERIMENTAL STUDY ON THE IDEALISED VORTEX SYSTEM OF A NOVEL ROTOR BLADE TIP

by

C.M. Copland, F.N. Coton, R.A.McD. Galbraith

Department of Aerospace Engineering,
The University of Glasgow,
Glasgow, G12 8QQ
Scotland

Abstract

Experiments have been conducted to investigate the flow field associated with two co-rotating vortices which represent the idealised vortex system associated with a novel rotor blade tip planform. These vortices were generated by two rectangular NACA 0015 half wings positioned upstream of the working section of a low speed wind tunnel. Hot-wire measurements were conducted downstream of the generators using X-wire probes to document the strength, position and size of the vortices. A numerical model was utilised to provide an accurate means of determining vortex strength, position and size. Finally, the model was successfully extended to consider the rotation of the vortex system.

Nomenclature

a	General constant
c	Vortex generator chord.
n	General constant
r	Radial distance, m .
r_c	Vortex core radius, m .
\bar{r}	Non-dimensional radius.
u_θ	Tangential velocity, ms^{-1} .
\bar{u}_θ	Non-dimensional tangential velocity.
u, v	Vertical and Horizontal velocity components respectively, ms^{-1} .
x, y	Measurement grid co-ordinate system.
Γ	Vortex circulation, m^2s^{-1} .

Introduction

The association of vortex systems with the production of aerodynamic forces is, for most aeronautical applications, well understood. In some cases, however, such as rotary wing aircraft, the vortex systems are particularly complex and highly unsteady and their interaction with the rotating lifting surfaces creates additional undesirable effects such as noise emission and structural vibration. On a helicopter, this phenomenon is termed Blade-Vortex Interaction (BVI)

and occurs when the tip vortices trailed from the rotor pass close to, or impact directly with, any of the blades in the main rotor or tail rotor systems. In some flight conditions BVI can be particularly severe and is manifest as high-frequency impulsive loads on the rotor blades.

The importance of BVI has been recognised for many years and has been the focus of several experimental¹⁻⁴ and numerical^{5,6} studies. Of these, most have concentrated on main rotor BVI although some, notably the in-flight study of Ellin⁷, have considered the interaction of the main rotor wake with the tail rotor.

Experimental studies have been predominantly wind-tunnel based and have utilised a variety of test geometries to create the BVI phenomenon. Early studies attempted to isolate single interactions in the hope that a clear description of the process would be forthcoming. Unfortunately, these tests were often hampered by problems associated with vortex generation or poor measurement resolution. In recent years, improvements in instrumentation technology have allowed more detailed studies of BVI, both as an isolated phenomenon and also in the full rotor domain to be conducted. Of particular relevance to the present study is the surface pressure measurement and flow visualisation work of Kokkalis et al.¹ and, subsequently, Horner et al.^{2,3,4}. In these tests, a vortex generator was located upstream of a single-bladed rotor in the working section of a low-speed wind tunnel. During the interaction of the vortex with the rotor blade, unsteady surface pressures were measured and Particle Image Velocimetry was used to obtain quantitative flow field information.

In most of the work described above, the emphasis has been on developing an understanding of BVI events associated with a conventional helicopter blade tip. Recently, however, several novel blade tip designs such as the BERP tip, have been developed and have entered service on operational aircraft. It has been documented by Scott et. al.⁸ that this tip may generate two trailed vortices at moderate-to-high incidence (fig. 1) the outboard vortex being relatively stronger than

the inboard which is of opposite sense. Lowson⁹ also stated that this tip reduces the noise in low speed descent, where BVI is predominant.

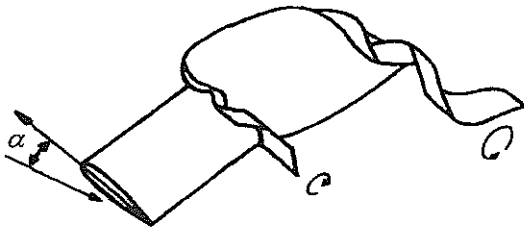


Fig.1- Illustration of the vortical flow field associated with the BERP tip at high incidence (ref. 8).

It has also been possible to consider the design of tip platforms specifically to modify the tip vortex structure in a manner which potentially reduces the severity of the associated BVI events. One such design is the so-called 'Vane-Tip' (fig. 2) proposed by Brockelhurst and Pike¹⁰ and which distributes the vorticity at the blade tip as a pair of co-rotating vortices. Theoretically, this has the potential to considerably reduce the severity of individual BVI events thus producing a corresponding reduction in noise¹¹. Unfortunately, little is known about the temporal and spatial development of two such closely spaced trailed vortices and so it is difficult to assess the actual effect which such a tip design would have.

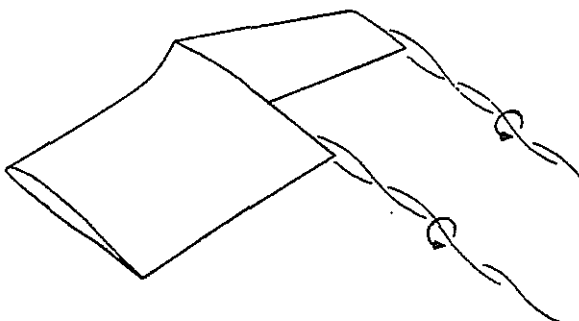


Fig.2- Illustration of the vortical flow field associated with the Vane Tip¹⁰.

In an attempt to alleviate this problem, the present study examines the generation and subsequent behaviour of a vortex pair in a wind tunnel environment. It is shown that the vortices can be modelled accurately using a simple two-dimensional core model and that their rotation can be predicted in a straightforward manner. The results of the study will, subsequently, be used in preparation for a BVI test series which will be conducted in the same facility as that used by Horner et al.^{2,3,4}.

Methods

The experiments were conducted in the 1.15m x 0.85m low speed wind tunnel of the Department of Aerospace Engineering, Glasgow University. This is a closed return facility capable of speeds up to 33 m/s. The test section length is 1.8m. The tunnel is equipped with an automated two component traverse which can be wall mounted vertically or on a support structure horizontally. The traverse is actuated via stepper motors controlled through a data acquisition board by software written under Labview. The positional error of the traverse is of the order of 0.5%.

The vortex generators, in this investigation, consisted of two rectangular cantilever wings of chord 0.1m, one mounted from the floor of the wind tunnel and the other from the roof (fig. 3). The length of each wing, 0.4m, was almost half of the tunnel height at the generator location such that, when the wings were exactly aligned, they formed a near continuous vertical blade. In a manner similar to refs 1-4, a single vortex could be generated at the junction of the two wings by setting the wings at opposite incidence to each other. Similarly, twin trailed vortices could easily be produced by introducing lateral spacing of the two wings.

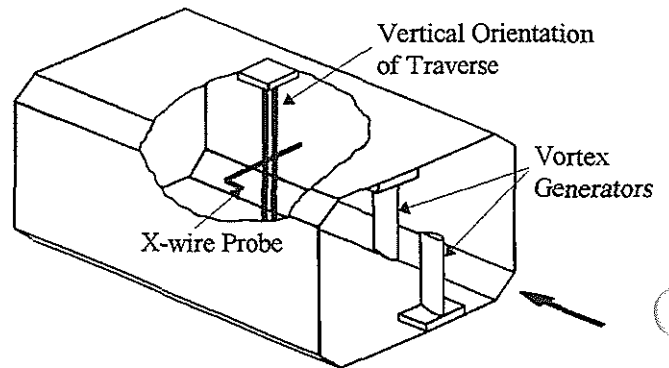


Fig.3- Illustration of Experimental Set-Up.

The wings were manufactured from wood and the base plates from aluminium. Each blade was secured to its base plate by a locking mechanism which passed through the $\frac{1}{4}$ c position of its NACA 0015 aerofoil section. The base plates were then surface mounted to the floor and roof of the tunnel. Looking upstream, the vortex generator mounted on the floor of the tunnel was positioned left of the centre-line and the top generator on the right. The base plates allowed each blade to be varied laterally from the centre line of the tunnel by approximately 1.5 chord lengths. A blade incidence variation of $\pm 12^\circ$ could be achieved in 2° increments.

Measurements of the magnitude and associated direction of the time-dependant velocity vector were obtained using a cross-wire probe connected to a TSI IFA-300 three-channel constant temperature anemometer system. For a single cross-wire, the maximum sampling rate for this system is 400 kHz. The cross-wire probes used in this study were DANTEC 55P61 probes. The sensor wires on these probes are 5 μm diameter platinum plated tungsten wires with a length/diameter ratio of 250, which form a measuring volume of approximately 0.8mm in diameter and 0.5mm in height. The wires are orientated perpendicular to each other corresponding to 45 degrees from the freestream direction which gives the best angular resolution. An additional temperature probe was used to correct the anemometer output voltages for any variation in ambient flow temperature.

For calibration, an open jet vertical wind tunnel with a maximum operating velocity of 43 m/s was used. A support allowed the sensors of X-wire probe to be rotated by $\pm 30^\circ$ in the plane of the sensors. Variation of the flow velocity and yaw angle then enabled the coefficients of the effective velocity method to be determined. As with all measurements utilising delicate wire sensors, breakage was a common occurrence. An in-house repair kit allowed the probe to be fixed quickly and so minimised down time in this event.

In order to fully determine the lateral and vertical components of velocity, the probe had to be rotated around its axis by 90 degrees to adjust the wire plane (horizontal and vertical) against the main flow direction. Thus, two traverse sweeps were necessary to obtain the vertical (u) and lateral (v) components respectively. The streamwise component of velocity was thus acquired twice but this component was strongly effected by the unmeasured velocity component which is perpendicular to the wire plane. This transverse contamination, as noted in ref. 12, does not adversely effect the other in-plane measured velocity component which is of primary interest.

Description of Tests

Flow field measurements were conducted in a plane perpendicular to the freestream direction for a constant freestream velocity of 30 m/s. This gives a Reynolds number of approximately $Re=2.1 \times 10^5$ based on the chord of the vortex generator. On the basis of previous studies, this Reynolds number is above the threshold below which low Reynolds number effects become significant on the NACA 0015 section.

The sampling frequency for each channel was set at 2 kHz. The anemometer signals were then

automatically low pass filtered at 1 kHz before digitising to counter aliasing. The sampling time for each point was 2 seconds which enabled a single grid traverse to be acquired in 2 hours.

The measurement grid size varied depending on the orientation of the traverse and was dependent on the position of the traverse with respect to the walls of the working section. A grid size of 100mm horizontal and 200mm vertical was attainable with the traverse in a vertical orientation. Horizontally, the maximum grid size was 160mm horizontally and 160mm vertically. Measurements were conducted every 10mm and so 231 points and 289 points were acquired for the vertical and horizontal traverse orientations respectively.

Table 1 documents the tests conducted. Initial tests were carried out to investigate the general flow field associated with two co-rotating and counter rotating vortices as well as the single vortex. These tests were conducted at two downstream positions corresponding to 2.5c and 6c behind the trailing edge of the vortex generators. The vortex generators were also varied to generate different sense vortex rotation in the single and twin vortex cases.

Further tests were then implemented at the optimum settings which generated a 0.5c separation of vortex cores - as produced by the Vane Tip. The first test was an investigation of the variation of blade incidence at 4.3 chord lengths downstream of the trailing edge. Detailed flow field measurements were then conducted at 10 degrees incidence from 0.1c to 10c downstream. Finally an investigation into the effects of generator blade separation was carried out. Blade separation was varied from 0c to 1c with measurements at 4c and 8c downstream of the generator.

Table 1 - Chronological list of tests conducted in the 1.15m x 0.8m wind tunnel.

<i>Test Conducted</i>	<i>Description of Test</i>
<i>General Blade Orientations</i>	Single and co/counter rotating twin vortex measurements conducted at 2.5c and 6c downstream of T.E.
<i>Incidence Variation</i>	2-12 degree incidence variation at 4.3c downstream. Blade separation of 0.5c between $\frac{1}{4}$ c positions
<i>Downstream Position</i>	Variation in downstream measurement position 0.1c-10c. Vortex Generator separation held constant at 0.5c between $\frac{1}{4}$ c positions. 10 degrees incidence.
<i>Blade Separation</i>	Variation of $\frac{1}{4}$ c separation position from 0c to 1c every 0.25c. Measurements conducted at 4c and 8c downstream of T.E. 10 degrees incidence.

Model Formulation

As with all measurements in vortex flows, a consistent method must be used to determine the relative parameters of the flow field. Previous investigations have utilised an analytical vortex model to curve fit the two dimensional tangential velocity component. These models are usually derived from fixed wing studies. This is perfectly satisfactory for single vortex configurations but when dealing with two vortices, which are closely spaced, the tangential component of velocity varies significantly between the cores. The two primary factors for determining the vortex strength, core size and maximum (tangential) velocity, are difficult to predict when dealing with a discretised grid. Measurements may not provide values for the maximum velocity and so underestimate the vortex strength and overestimate core size.

For a single vortex the rule that the tangential velocity is proportional to $1/r$ must break down for small values of r to avoid unphysical singularities on the axis itself. The fluid velocity can never be infinite in the real world, and in so far as it reverses direction between two points which lie close to the axis but on opposite sides, the change cannot be a discontinuous one. Thus every free vortex line must have a core of some sort.

The immense complexities associated with concentrated vortices have prevented the derivation of a theoretically rigorous vortex model which describes the phenomena in every respect. For this reason several empirical formulae for the tangential velocity have been used by many to study different aspects of concentrated vortices. The best known among these are the Rankine and Lamb-Oseen¹³ models. The Rankine vortex rotates as a solid body within its core and is characterised by a potential flow outside, i.e. all the vorticity is confined to the core region.

Vatistas¹⁴ et. al. proposed an equation which represents a series of general velocity profiles for rectilinear vortices. This core model links Rankine's model and the Scully¹⁵ model and has been compared, in ref. 14, to Burgers Model. The tangential velocity in the core is expressed by Vatistas in non-dimensional terms as

$$\bar{u}_\theta = \frac{\bar{r}}{(1 + \bar{r}^{2n})^{1/n}}$$

with a maximum of

$$\bar{u}_\theta = 2\pi r_c u_\theta / \Gamma$$

$$\bar{r} = r/r_c$$

The Scully model corresponds to $n=1$ and the Rankine model to $n \rightarrow \infty$ where n and a are integer constants.

Since the above equation must have a maximum at $\bar{r} = 1$, a has to be equal to 2

Leishman^{16,17} et. al. utilised a specific form of this model in rotor vortex measurements. They determined the tip vortex profile for a rotating blade could be approximated (dimensionally) as

$$u_\theta = \frac{\Gamma}{2\pi r} \cdot \frac{r^2}{\sqrt{r^4 + r_c^4}}$$

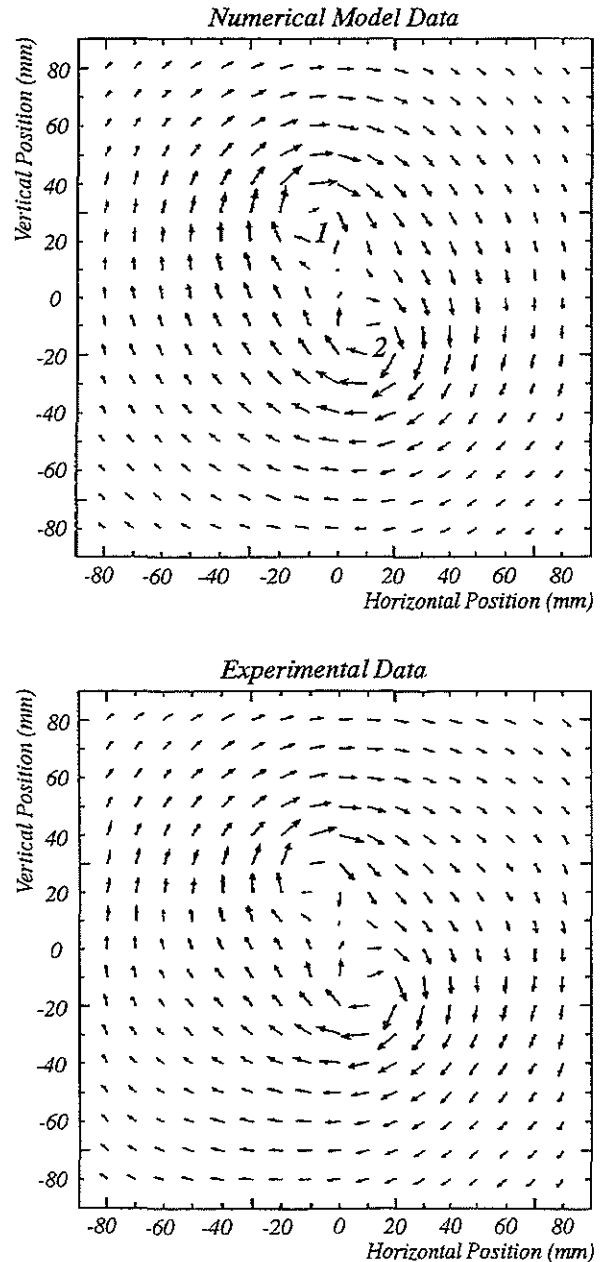


Fig.4- Comparison of Vector plots from Numerical Model and Experimental Data.

Numerical models can be used in conjunction with experimental data to provide a means to

determine two dimensional parameters which could represent the two measured in-plane velocity components. The Scully model was chosen due to its common use in curve fitting experimental single vortex data^{16,17}.

Each of the Scully vortices induces a velocity component on each of the discrete grid points. This velocity component is derived from the Biot-Savart law applied in two dimensions. At these points the tangential velocity from each vortex is decoupled into the appropriate grid horizontal and vertical velocity components which are then superposed. The numerical model grid and experimental grid are of the same dimensions which enabled a direct point for point comparison to be conducted.

As a prerequisite for the numerical model, initial values for the position (x and y co-ordinates), core size (r_c) and vortex strength (Γ) must be specified for the two vortices. These parameters are then altered to obtain a suitable fit for the majority of the horizontal and vertical mean velocity components acquired experimentally. Two sets of experimental data (one for each in plane velocity component) are fitted to one set of numerical data. There were slight differences between the two separately acquired components in some configurations (as can be seen from Fig. 5). This was primarily due to vortex meander and probe interference. In some cases, however, this proved insignificant compared with the discrepancies attributable to the highly three-dimensional nature of the flow field. Outside the cores, the two wake structures from the vortex generators were dominant flow features. These errors were localised to specific regions of the grid for the vertical velocity component when measurements were conducted close to ($<5c$) the generator blades. An adequate curve fit to both sets of data (u, v) could, however, be determined from the horizontal component of velocity.

Once the fitting parameters had been obtained for all the experimental data in the cross-flow plane, a quasi three-dimensional adaptation was used to predict the rotation of the vortex system as it travelled downstream. This model utilised an Adams-Bashforth multi-step integration based on the two velocity components. In this scheme, data from a measurement plane close to the vortex generator were used as initial conditions for the 3D model. By consideration of the induced flow field it was then possible to apply the technique to predict the orientation of the vortices further downstream. This proved successful with errors primarily arising from the interference effect of the traverse and the time dependant change in vortex size and strength.

Results and Discussion

Comparisons of the experimental data with the numerical model are provided in Figs. 4 and 5 for the same case. Figure 4 depicts the flow field associated with the optimum configuration to produce a similar flow to that generated by the Vane Tip. For this case, each vortex generator was set at an incidence of 10 degrees with a $0.5c$ separation between the $\frac{1}{4}c$ locations of the aerofoils. In this configuration, the

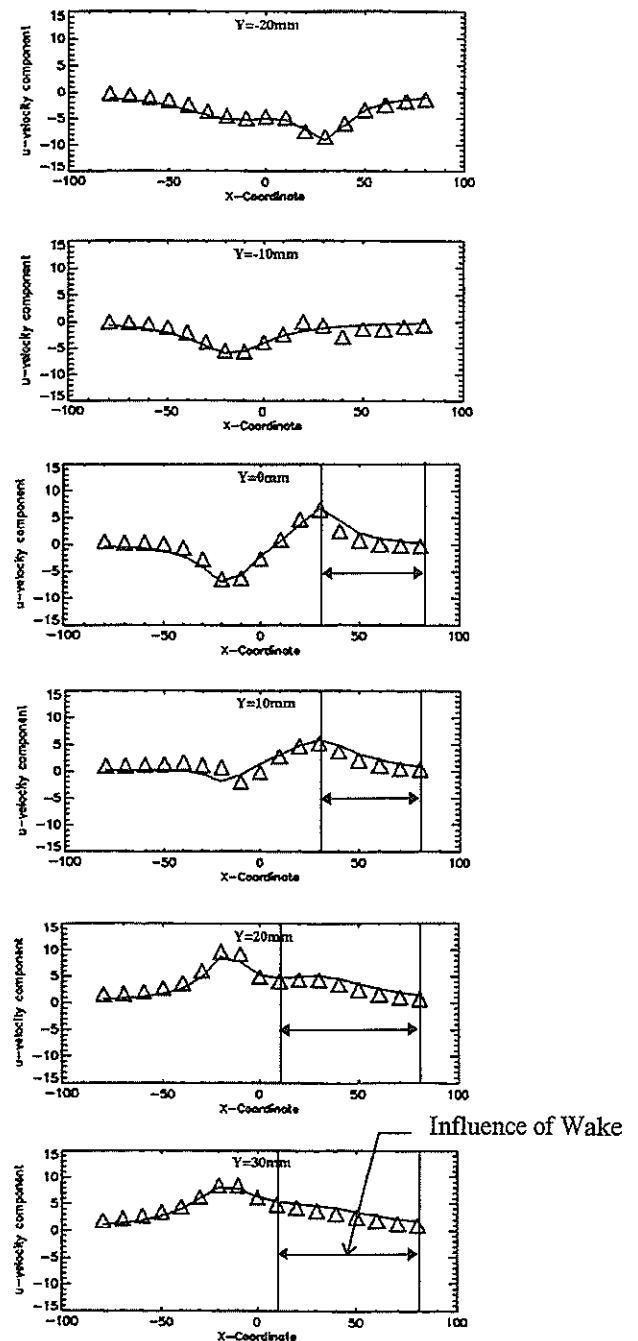


Fig.5a- Comparison of experimental u (vertical) velocity component with numerical model.

trailing edges of the vortex generators were pointing towards the tunnel walls (as opposed to pointing towards the centre line). The vector plots are shown looking upstream and clearly illustrate the level of correlation between the experiment and numerical model. The vortex parameters were obtained from the numerical model (line in Figs. 5a & b). These correspond to, for position 1 in Fig. 4 (where the vortex originates from the lower vortex generator), a strength of $0.95 \text{ m}^2\text{s}^{-1}$, vertical position $x=0.03\text{m}$ and horizontal

position $y=-0.01\text{m}$ and, for position 2, a strength of $1.0\text{m}^2\text{s}^{-1}$ at $x=-0.017\text{m}$, $y=0.012\text{m}$. Both vortices have a core radius of 0.01m .

With a single finite wing, it is expected that the vortex will roll-up inboard of the tip. However, in the twin vortex configuration documented here, the second vortex induces a velocity which acts against this inboard motion. When the trailing edges of the blades are oriented towards the centre line (reversing the sense of rotation) the induced velocities are in the same direction as the inboard roll-up.

When consideration is given to the movement of the wake from the vortex generators, a configuration with the trailing edges oriented towards the tunnel walls results in the wake being convected away from the centre of the tunnel. Correspondingly, the wake is convected toward the centre of the tunnel and the other vortex when the blades are oriented towards the centre-line. For BVI investigations it is inadvisable to have the wake structure convecting across the interacting plane as this may have a significant effect on the BVI event.

In Figs. 5a and 5b the individual comparisons of the u (vertical) and v (horizontal) components are presented for $Y=-20$ to 30 mm (horizontal positions). Each individual plot corresponds to a vertical slice of the grid and the plots depicted in Figs 5a and 5b correspond to the regions of highest velocity gradients associated with the core region. As can be seen from the figures, there is a discrepancy in the u velocity magnitudes (Fig. 5a) at positive x -coordinate values and especially for $Y=0-30\text{mm}$. This discrepancy is evident for two localised regions in the complete grid ($Y=-80$ to 80mm) and is due to the momentum deficit in the wake behind each generator. The region does grow due to the reduction in velocity when moving away from the core. All the regions are of positive x and positive y -coordinates corresponding to a location on the right and above the centre line. This is the region of the upper vortex generator. A corresponding effect is noted in the measurement plane for the lower generator.

The v -component is not as adversely affected by the generator wake and so the strengths of the vortices, in this case, were determined from the v -components. The general distribution of velocity through the vortex cores, and in the irrotational region outwith the cores, is very good. The interference problem with the wake reduces with increasing distance from the generator.

It should be noted that when surface fitting the two components, initially the vortex strength is varied to obtain the correct irrotational velocity

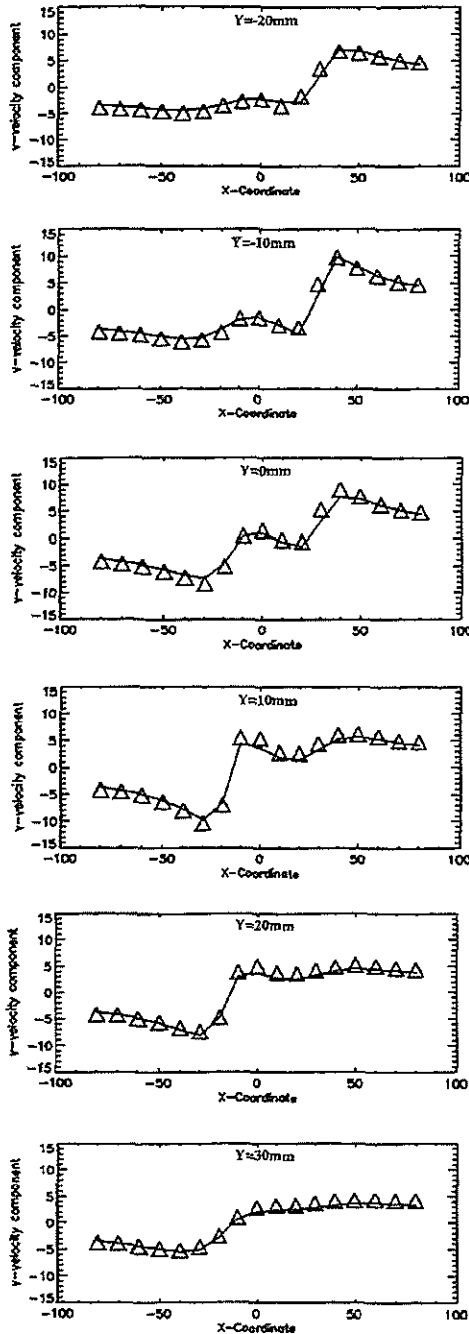


Fig.5b- Comparison of experimental v -velocity component and numerical model.

magnitudes and then the core size is varied to alter the velocity gradients for each core. The curve fit is highly sensitive to the vortex position (x,y co-ordinate specification) but not to vortex strength.

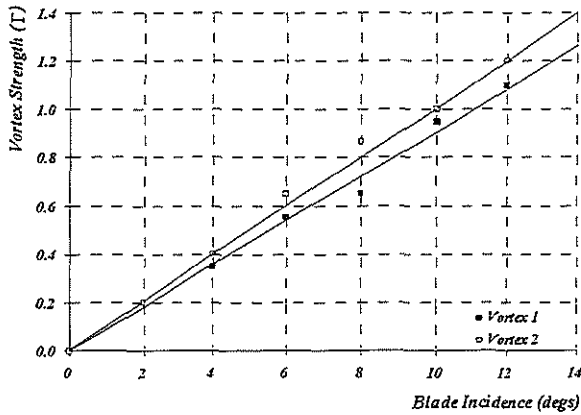


Fig.6- Variation in vortex strength with change in incidence at 4.3c downstream of trailing edge.

In Fig. 6 the vortex strengths produced by each blade of the generator are plotted against blade incidence setting. The measurement position was 4.3 chord lengths downstream of the trailing edge and each vortex generator was set at an incidence of 10 degrees with a 0.5c separation between the $\frac{1}{4}c$ locations of the aerofoils (same parameters for Figs. 7 & 8). As may be expected from the Kutta-Joukowski theorem, the strength was found to vary linearly with incidence at moderate incidence settings. There was, however, a consistent difference between the strength of the vortices trailed from each blade of the generator. This was apparently due to flow angularity in the test section of the wind tunnel.

Figure 7 depicts the variation in vortex core separation with respect to blade incidence. The graph shows an almost linear relationship with the vortices moving closer together as the incidence is increased. This relationship initially appears surprising since the increase in blade incidence also corresponds to an increase in trailing edge separation. For example, a blade incidence of 2 degrees corresponds to a trailing edge separation of 0.552c and a blade incidence of 10 degs corresponds to a trailing edge separation of 0.76c. Obviously, the initial development of the twin vortex system cannot be considered purely on the basis of the generator geometry. Consideration must also be given to the fluid dynamic behaviour at the two wing tips.

As the blade incidence is increased, there is a corresponding increase in mass flow over the blade tips. On a single finite wing, this has the effect of moving the vortex roll-up location in-board and

slightly raising the height of the core above the trailing edge. In the present case, the situation is complicated by the inevitable confluence of the two wing-tip flows. It has been established that one consequence of this is a

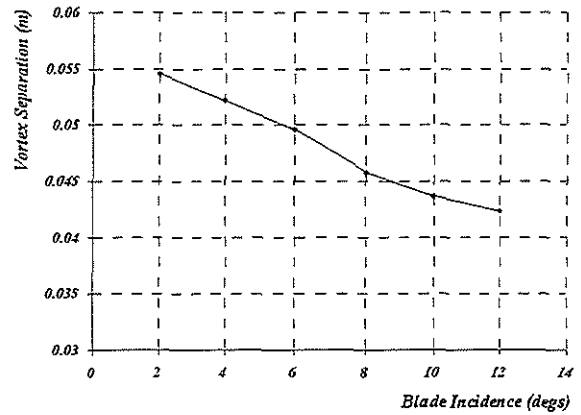


Fig.7- Variation in vortex core separation with a change in incidence at 4.3c downstream.

reduction in the inboard movement of the tip vortices due to the induced effect of one tip vortex on the other. Given this behaviour, momentum considerations would suggest that this should be accompanied by an increase in the distance between the vortex and the suction side of the trailing edge in the direction normal to the chord line. Further, it would be expected that this distance would progressively increase with blade incidence in a manner which is consistent with the results of Fig.7. Also, there is an initial inward convection of the vortices between 0.1 and 2 chord lengths downstream of the trailing edge which is illustrated in Figure 13. This was detailed for one incidence case only, where the blades were at 10 degrees incidence with a separation of 0.5c. It is possible that this inward convection is related to vortex strength and hence incidence. If the incidence is reduced there should be a reduction in the inward convection and so an increase in vortex separation as shown in Fig.7.

In Fig. 8 the variation in core size with incidence is presented. It may be observed that, over the incidence range considered in this study, the core size was found to be insensitive to the blade incidence setting. This result is interesting, when taken together with Fig. 9 which documents the growth of the core radius with downstream position. Clearly the rate of growth is approximately linear with a core radius of 0.004m (0.04c) at 0.1 chords behind the trailing edge growing to 0.017m (0.17c) at 10 chord lengths downstream. It is interesting to note that these two results suggest that regardless of blade setting, the growth of the vortex cores will be linear and the size of

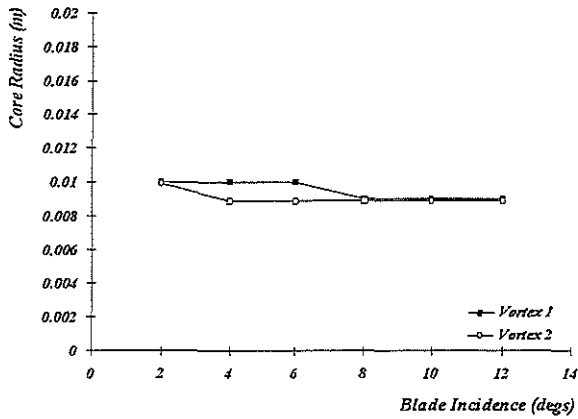


Fig 8- Variation in core size with a change in incidence at 4.3 chord lengths downstream.

the core will be consistent with Fig. 9. It is inevitable that the test Reynolds number will influence the core size and its rate of growth. Nevertheless, the result presented above has implications for wind tunnel based BVI tests which aim to reproduce core sizes of equivalent non-dimensional scale to those anticipated at full scale. Clearly, the distance between the point of generation and the interaction location must be chosen carefully.

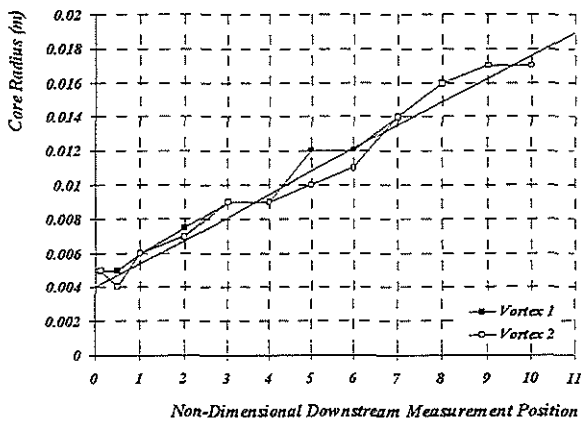


Fig 9- Variation in core radius with downstream measurement position.

In Fig. 10 the variation in vortex separation distance with downstream measurement position is shown. Here, the blade were held at a constant incidence of 10 degrees with a blade separation of 0.5c between 1/4 c locations (same parameters for figs 9 & 11). There is an initial reduction of the core spacing from just over 0.06m to approximately 0.05m within 2 chord lengths. Further downstream the core separation varies slightly and this can be attributed to the interference effect of the horizontally mounted traverse. This interference effect causes the vortex, which is convected downwards (towards the traverse), to be

forced toward the other vortex and so reduce the spacing. This occurs when the vortices are vertically oriented to one another between 5c and 6c downstream. Subsequently, as the vortices convect horizontally away from each other the spacing increases before returning to the general downward trend of the curve. Nevertheless, this apparent reduction in the separation distance is very slow and the vortices maintain their approximate 1/2 chord spacing throughout the graph.

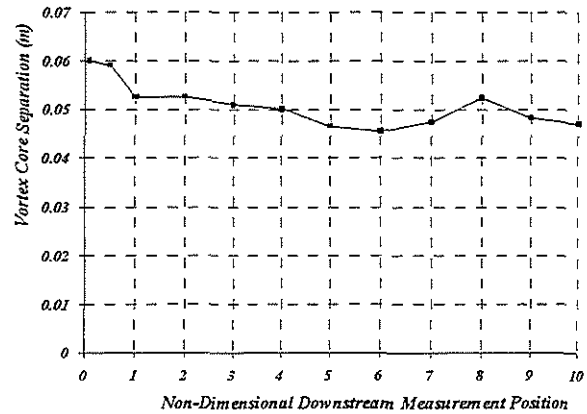


Fig 10- Variation in vortex separation with downstream measurement position.

Figure 11 illustrates the growth in vortex strength with downstream position. Here, there is an initial growth in vortex strength up to approximately 4c. This corresponds to the growth in core size downstream illustrated in Figure 9. This behaviour is due to the vorticity from the wake rolling up into the vortex. After 4c, however, the cores are fully rolled up and the core strength remains constant whilst the core radius continues to increase. This is associated with a redistribution of vorticity within the core, through

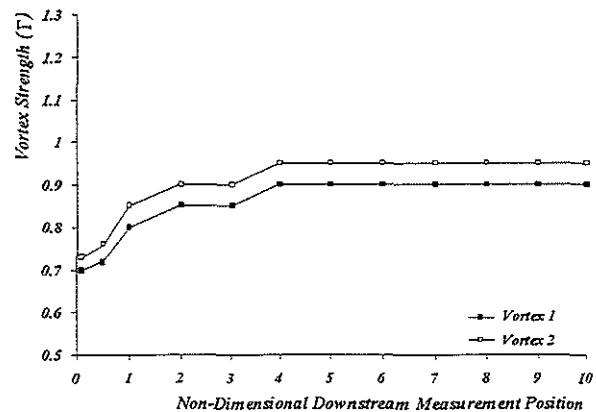


Fig 11- Variation of vortex strength with downstream measurement position.

diffusion, resulting in an enlargement of the core radius.

As may be observed in Fig. 12, the variation of vortex separation with generator blade spacing is approximately linear when measured at 4 chord lengths downstream. However, at 8 chord lengths, there is a dramatic change in vortex separation distance for 0.25c blade separation case. The behaviour illustrated for the 0.25c blade separation case is indicative of vortex merging. Rossow^{18,19} documented that vortex merging is dependent primarily on vortex core diameter and vortex separation distance. When the ratio of separation distance to vortex core diameter is approximately 1.9 the two cores will merge downstream to form one vortex.

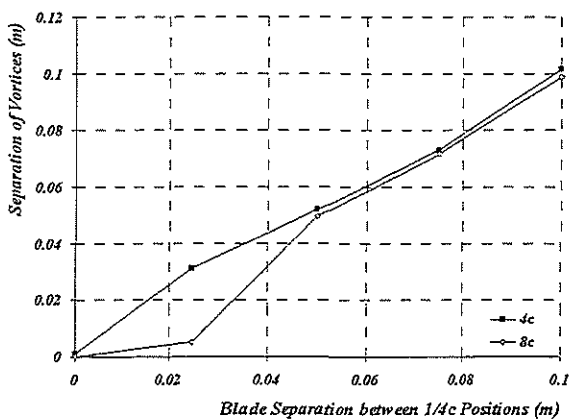


Fig.12- Variation of vortex separation with respect to blade separation for downstream measurements positions of 4c and 8c.

Based on the core radius documented in Fig. 9 for 4c, the ratio of core separation (0.025m) to core diameter (0.018m) is approximately 1.4 and the vortices, at this location, should be in the process of merging as this value is below the threshold for vortex merging to begin. At 8 chord lengths downstream the vortices are virtually completely merged and so the rapid formation of the single vortex agrees with the Rossow condition.

There is a slight discrepancy between the vortex separation depicted in Figs. 10 and 12 for 8 chord lengths downstream, 0.5c blade separation. The discrepancy results from the difference in individual vortex positions, which is less than 2mm. These two investigations were conducted independently. In Fig. 10, the blades were set at the required incidence and spacing and not altered when the downstream investigation was conducted. However, in the blade separation investigation (Fig.12) the blades were altered significantly between individual measurements which may account for this slight discrepancy.

In Figure 13 the spatial evolution of each vortex is plotted with respect to the centre line of the tunnel (looking upstream). The figure illustrates a significant initial inward convection of the two vortices with a slight rotation before the vortex assumes the typical full rotational behaviour expected. This inboard convection is consistent with the reduction in core separation with increasing blade incidence discussed in relation to Fig. 7. Also illustrated in this figure is a comparison between the experimental vortex trajectory and that predicted from the quasi three dimensional numerical model. The initial inputs to the model were the vortex strength, position and size determined from experiment at two chord lengths downstream. This is the first position which is outwith the initial inward convection region.

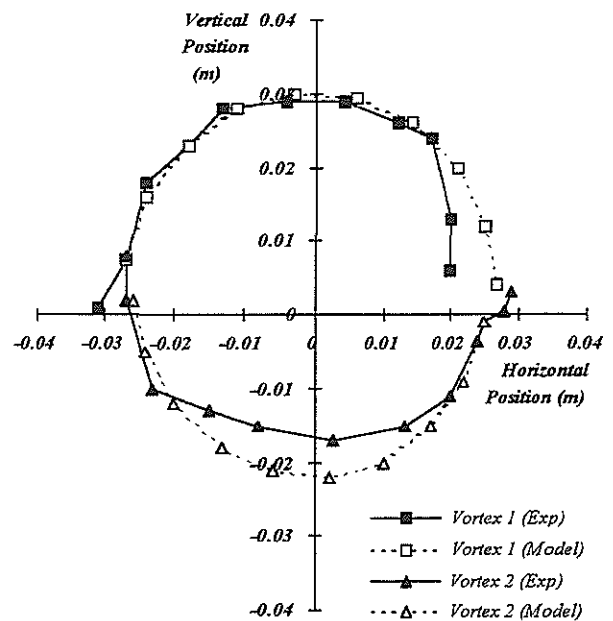


Fig.13- Location of twin vortices with respect to test section centre for variation in downstream position and comparison with numerical model.

At two chord lengths the vortex has not completely rolled up and so the vortex strength is slightly underestimated. This reduced strength of the vortices was investigated by using input parameters at 3 and 4 chord lengths downstream for comparison with the case presented. No appreciable difference was noted. As can be seen from the figure, vortex 1 follows the theoretical trajectory very well and the predicted locations up to 7 chord lengths are satisfactory. However, the cross-flow velocities recorded at nine and ten chord lengths downstream were low and the vortex cores were particularly diffuse. This made accurate determination of the x-axis (horizontal) core locations very difficult.

The trajectory of vortex 2 is, unfortunately, significantly different from that predicted by the numerical model. In these experiments the traverse was oriented horizontally and rested below the centre line of the wind tunnel. It is believed that vortex 2 was influenced by a vertical velocity component created by the blockage of the traverse which, on the right of Fig. 13, acted against the induced velocity from vortex 1 and correspondingly acted with the induced velocity on the left. Despite this the lateral movement of the vortex is well predicted.

Conclusions

A study of the flow field created by a twin vortex generator has been conducted. It has been demonstrated that the cross-flow created by the resulting vortex system can be adequately represented by a simple vortex core model. On the basis of this model, the strength, growth, lateral spacing and rotation of the vortex system were studied. It was found that the core size of the twin vortices grew almost linearly with downstream distance while the strength remained constant. The spacing between the two cores remained almost constant with only a slight decrease as the downstream distance increased.

Finally the rotation of the vortex system was modelled by a straight forward consideration of the induced velocity field. Generally, good agreement with experiment was obtained despite the influence of interference effects on the experimental data.

Acknowledgements

The authors would like to acknowledge the support of the British Ministry of Defence through the Defence Evaluation Research Agency (DERA). The work was funded by the DERA under extra-mural agreement ASF/2163U.

References

1. Kokkalis A., "An Experimental Investigation of Parallel Blade-Vortex Interaction for a NACA00015 Airfoil", *PhD Dissertation, University of Glasgow, Dept. of Aerospace Eng.*, 1988.
2. Horner M.B., Saliveros E., Galbraith R.A.McD., "An Experimental Investigation of the Oblique Blade-Vortex Interaction", *17th European Rotorcraft Forum, Berlin, Germany, Sept. 1991.*
3. Horner M.B., Stewart J.N., Galbraith R.A.McD., Grant I., Coton F., Smith G.H., "Preliminary Results from a Particle Image Velocimetry Study of Blade-Vortex Interaction", *19th European Rotorcraft Forum, Cernobbio, Italy, Sept. 1993.*

4. Horner M.B., Stewart J.N., Galbraith R.A.McD., Grant I., Coton F., "An Examination of Vortex Deformation during Blade-Vortex Interaction Utilising Particle Image Velocimetry", *19th Congress of the International Council of the Aero. Sciences, Anaheim, California, Sept 1994.*
5. Coton F.N., De la Iglesia F., Galbraith R.A.McD., Horner M.B., "A Three-Dimensional Model of Low Speed Blade-Vortex Interaction", *20th European Rotorcraft Forum, Amsterdam, The Netherlands, Oct 1994.*
6. Padakannaya R., "The Vortex Lattice Method for the Rotor-Vortex Interaction Problem", *NASA CR-2421, July 1974.*
7. Ellin A.D.S., "An In-Flight Investigation of Lynx AH Mk5 Main Rotor/Tail Rotor Interactions", *19th European Rotorcraft Forum, Cernobbio, Italy, Sept. 1993.*
8. Scott M.T., Sigl D., Strawn R.C., "Computational and Experimental Evaluation of Helicopter Rotor Tips for High-Speed Flight", *J.Aircraft 28, 403-409, June 1991.*
9. Lowson M.V., "Progress Towards Quieter Civil Helicopters", *Aero. J. , 209-23, June/July 1992.*
10. Brocklehurst A., Pike A.C., "Reduction of B.V.I. Noise Using a Vane Tip", *A.H.S. Aeromechanics Specialists Conf., San Francisco, Jan. 1994.*
11. Tyler D.J., Vincent A.H., "Future Rotorcraft Technology Developments", *Aero. J., 451-60, Dec.1996.*
12. Clausen P.D., Piddington D.M., Wood D.H., "An Experimental Investigation of Blade Element Theory for Wind Turbines - Part 1. Mean Flow Results", *J. Wind Eng. Ind. Aero. 25, 189-206, 1987.*
13. Lamb H., "Hydrodynamics", 6th Edition, Cambridge University Press, 1932.
14. Vatistas G.H., Kozel V., Mih W.C., "A Simpler Model for Concentrated Vortices", *Exp. Fluids 11, 73-6, 1991.*
15. Scully M.P., "Computation of Helicopter Rotor Wake Geometry and its Influence on Rotor Harmonic Airloads", *ASRL TR-178, M.I.T., March 1975.*
16. Leishman J.G., Baker A., Coyne A., "Measurements of Rotor Tip Vortices Using Three-Component Laser Doppler Velocimetry", *J. American Helicopter Soc. 41, 342-353, Oct. 1996*
17. Han Y.O., Leishman J.G., Coyne A.J., "Measurements of the Velocity and Turbulence Structure of a Rotor Tip Vortex", *ALAA J. 35, 477-85, Feb.1997.*
18. Rossow V.J., "Convective Merging of Vortex Cores in Lift-Generated Wakes", *J. Aircraft 14, 283-290, 1977.*
19. Rossow V.J., "Prospects for Destructive Self-Induced Interactions in a Vortex Pair", *J. Aircraft 24, 433-40, 1987.*